

Pressure-tuning of the thermal conductivity of a layered crystal, muscovite

Wen-Pin Hsieh,^{1,5,*} Bin Chen,² Jie Li,² Pawel Koblinski,³ and David G. Cahill^{4,5}

¹*Department of Physics, University of Illinois, Urbana, Illinois 61801, USA*

²*Department of Geology, University of Illinois, Urbana, Illinois 61801, USA*

³*Department of Materials Science and Engineering, Rensselaer Polytechnic Institute,
Troy, New York 12180, USA*

⁴*Department of Materials Science and Engineering, University of Illinois, Urbana,
Illinois 61801, USA*

⁵*Frederick-Seitz Materials Research Laboratory, University of Illinois, Urbana, Illinois
61801, USA*

The physics of heat conduction in layered, anisotropic crystals is probed by measurements of the cross-plane elastic constant C_{33} and thermal conductivity Λ of muscovite mica as a function of hydrostatic pressure. Picosecond interferometry and time-domain thermoreflectance provide high precision measurements of C_{33} and Λ , respectively, of micron-sized samples within a diamond anvil cell; Λ changes from the

anomalously low value of $0.46 \text{ W m}^{-1} \text{ K}^{-1}$ at ambient pressure to a value more typical of oxides crystals with large unit cells, $6.6 \text{ W m}^{-1} \text{ K}^{-1}$, at $P=24 \text{ GPa}$. Most of the pressure dependence of Λ can be accounted for by the pressure dependence of the cross-plane sound velocities and elastic anisotropy.

Recently, ultra-low thermal conductivity—i.e., thermal conductivity Λ significantly lower than predicted by the model of the minimum thermal conductivity—was observed in disordered, layered crystals [1]. A subsequent theoretical study suggested that a high degree of elastic anisotropy plays a critical role in suppressing the thermal conductivity in the cross-plane direction [2]. Measurements of the thermal conductivity as a function of pressure enable a critical test of this idea by enabling a continuous tuning of the anisotropy of the elastic constants; typically, the softer elastic constant in the cross-plane direction of a layered crystal has a higher anharmonicity and therefore increases more rapidly with pressure than the stiffer in-plane elastic constants.

Low thermal conductivity in layered crystals may find applications in improving thermal barriers and materials for thermoelectric energy conversion [3-6]. We have chosen a prototypical layered crystal, muscovite mica, for these initial studies. Even though the layered structure of muscovite is not disordered, Λ in the cross-plane direction

is extremely small for an oxide, $0.46 \text{ W m}^{-1} \text{ K}^{-1}$ [7, 8], a factor of ≈ 2 smaller than the predicted minimum thermal conductivity in the cross-plane direction. The thermal conductivity at ambient pressure is also highly anisotropic; the in-plane thermal conductivity is $\approx 4 \text{ W m}^{-1} \text{ K}^{-1}$ [7].

To obtain high precision data for Λ at high pressures, an advance in experimental methods was required. The pressure dependence of the thermal conductivity of solids has been extensively studied at pressures up to $\approx 2 \text{ GPa}$ [9-13]. However, much higher pressures, $\approx 20 \text{ GPa}$, are needed to significantly alter the anisotropy of a layered oxide crystal. Studies of Λ up to or beyond 20 GPa are rare in the scientific literature and are essentially limited to studies of molecular crystals [14]; and relatively recent work applying the Ångström method within a 5000-ton multianvil apparatus [15] and flash diffusivity within a diamond anvil cell [16].

Here, we present our study of the cross-plane elastic constant C_{33} and thermal conductivity of an anisotropic layered crystal, muscovite mica, from ambient pressure to 24 GPa using optical pump-probe methods combined with the diamond anvil cell techniques [17]. Comparisons to a simple model show that elastic anisotropy plays a significant role in suppressing the cross-plane thermal conductivity of layered crystals.

A sheet of $\sim 20 \mu\text{m}$ thick muscovite mica, $\text{KA}_2(\text{Si}_3\text{Al})\text{O}_{10}(\text{OH})_2$ (grade V-1 from SPI

Supplies), was first coated with an Al film of ~ 80 nm thick and loaded, together with a small crystal of ruby, into a diamond anvil cell (DAC) with culet size of ≈ 500 μm and pressurized by high-pressure gas loading with Ar [18], see Fig. 1. Hydrostatic pressure was determined by ruby fluorescence [17]. The cross-plane thermal conductivity Λ of muscovite was measured at room temperature by time-domain thermoreflectance (TDTR) [19-21]. In the TDTR measurement, the output of a mode-locked Ti:sapphire laser was split into a pump beam, which heats the surface of the Al film on the muscovite sample, and a probe beam, which subsequently examines the resulting changes in reflectivity due to changes in temperature of the Al film [22]. The in-phase V_{in} and out-of-phase V_{out} components of the small variation of the reflected probe beam intensity that are synchronous with the 10 MHz modulation frequency of the pump beam were measured by a photodiode detector and rf lock-in amplifier. We found that the thermoreflectance of Al at 785 nm crosses through zero at $P \approx 6$ GPa [23]; we used a laser wavelength of 765 nm to obtain data near this pressure. (At 765 nm, the thermoreflectance of Al is zero near $P \approx 8$ GPa.)

To determine the cross-plane thermal conductivity of muscovite, we compared the ratio V_{in}/V_{out} as a function of delay time to calculations using a thermal model [24] that was modified to take into account heat flow into the muscovite as well as into the Ar

pressure medium [25]. The thermal penetration depth at the modulation frequency of the pump beam is 50-200 nm, small compared to the radius of the laser spot size, 7.5 μm , and heat flow is predominately one-dimensional in the cross-plane direction. Example data and fits to the thermal model are shown in Fig. 2(a).

The thermal model has many parameters—laser spot size, Al film thickness, thermal conductivity and heat capacity of each layer—but the thermal conductivity of muscovite is the only significant unknown. The thickness of Al was determined by picosecond acoustics. The pressure dependent thermal conductivity of Ar at room temperature was taken from recently published computer simulations [26]. Because the thermal conductivities of muscovite and Ar are relatively small, the thermal model is insensitive to the thermal conductance G of the Al interfaces; we fix $G=200\text{ MW m}^{-2}\text{ K}^{-1}$ for the Al/muscovite interface and scale the conductance of the Al/Ar interface by $G=70+5.2P$ $\text{MW m}^{-2}\text{ K}^{-1}$, where P is the pressure in GPa.

The heat capacities of Al, muscovite, and Ar at high pressures are not known; therefore, we estimate the pressure dependence of the heat capacities from data for the pressure dependence of the atomic density and elastic constants. Because of the relatively low Debye temperature of Ar, we fix the heat capacity per atom at the classical value: $C=1.36$, 1.86, and 2.16 $\text{J cm}^{-3}\text{ K}^{-1}$ at $P=2$, 10, and 20 GPa, respectively [27]. For Al, we assume

that changes in the specific heat at high pressure can be estimated from the ambient pressure specific heat at reduced temperature; for example, at 10 and 20 GPa, the Debye temperature of Al increases by 24% and 43% [28], respectively, and therefore we use the measured specific heats of Al at $T=242$ K and $T=210$ K to calculate the heat capacities at 10 GPa and 20 GPa. For Al, the pressure dependence of atomic density n is stronger than the pressure dependence of the specific heat and the heat capacity per unit volume of Al ($C=2.42$ J cm⁻³ K⁻¹ at ambient pressure) increases by 5% at 10 GPa and 9% at 20 GPa [29, 30]. For muscovite, we use data for the pressure dependence of the elastic constants of MgSiO₃ [31] to estimate the changes in the Debye temperature. (The temperature dependence of the specific heats of muscovite and MgSiO₃ are nearly identical over a wide temperature range [29].) By this calculation, the heat capacity of muscovite ($C= 2.3$ J cm⁻³ K⁻¹ at ambient pressure) increases by 9% at 10 GPa and 15% at 20 GPa. The density of muscovite (2.83 g cm⁻³ at ambient pressure) increases by 11.5% at 10 GPa and 20% at 20 GPa [32].

We measured the Brillouin frequency f of muscovite by picosecond interferometry [33, 34]; in a backscattering geometry, $f = 2Nv / \lambda$, where N is the index of refraction, v the longitudinal speed of sound, and λ the laser wavelength. Thermal expansion of Al created by heating by the pump laser pulses generates a strain pulse; interference of probe pulses

reflected from the strain pulse and the Al surface creates periodic oscillations of the in-phase signal V_{in} , see Fig 2(b). Figure 3(a) shows the pressure dependence of f . To determine the corresponding cross-plane elastic constant C_{33} , see Fig. 3(b), we calculated the pressure dependence of the density ρ from the equation of state of muscovite [32] and calculated the index N using the Lorentz-Lorenz formula $(N^2 - 1)/(\rho(N^2 + 2)) = A$, where A is a constant [35]. At ambient pressure, $N= 1.56$, $\rho= 2.83 \text{ g cm}^{-3}$, and $A= 0.114$; N increases by 4.8% at 10 GPa and 9% at 20 GPa.

We can not measure the pressure dependence of the in-plane elastic constant C_{11} in our apparatus but if we assume that $dC_{11}/dP \approx 4$, as suggested by data for MgSiO_3 [31], $C_{11}= 184 \text{ GPa} + 4P$ and $C_{33} \approx C_{11}$ at the upper-end of our pressure range, see Fig. 3(b). As muscovite is compressed, the decreasing interplanar distance increases the force constants of the interaction between the silicate layers [35].

Figure 4 shows the pressure dependence of the cross-plane thermal conductivity Λ of muscovite; Λ increases by a factor of ≈ 3 at a relatively modest pressure of 5 GPa and increases by a factor of ≈ 15 at 24 GPa. The measured thermal conductivity increases monotonically with pressure and therefore does not support a previous report of a crystal-to-amorphous transition in muscovite at $P \geq 20$ GPa [32].

We compare the thermal conductivity data to two simple models. First, we consider the

thermal conductivity in the relaxation time approximation, $\Lambda = C \langle v_z^2 \rangle \tau$, where C is the heat capacity per unit volume of the vibrational modes that contribute significantly to heat transport, τ is the relaxation time, and $\langle v_z^2 \rangle$ is the average of the square of the cross-plane components of the group velocities of the vibrational modes. If we assume that the heat capacity and relaxation time are weakly dependent on pressure, changes in Λ are only the result of changes in $\langle v_z^2 \rangle$.

In an anisotropic Debye model, the phonon dispersion is

$\omega^2 = (k_x c_x)^2 + (k_y c_y)^2 + (k_z c_z)^2$, where k_i and c_i are the wave vector and speed of sound along the i direction. The group velocity in the cross-plane direction is

$v_z = \partial\omega/\partial k_z$. With $c_x=c_y$

$$\langle v_z^2 \rangle = c_z^2 \int_0^{\pi/2} \frac{c_z^2 \cos^2 \theta}{c_x^2 \sin^2 \theta + c_z^2 \cos^2 \theta} \sin \theta d\theta. \quad (1)$$

To evaluate Eq. 1, we assume that the pressure dependence of c_x^2 and c_z^2 follows the pressure dependence of C_{11} and C_{33} . The pressure dependence predicted by Eq. 1 is indicated by the solid line in Fig. 4. This simple approach does not take into account changes in the average relaxation time with pressure but the good agreement between the data and the prediction of Eq. 1 suggests that most of the pressure dependence of Λ is accounted for by changes in the sound velocities and elastic anisotropy.

We note, however, that the Leibfried-Schlömann (LS) equation—often used to model

the pressure dependence of Λ —can also describe the data:

$$\Lambda = A \frac{V^{\frac{1}{3}} \omega_D^3}{\gamma^2 T}, \quad (2)$$

where V is the volume, ω_D the Debye frequency, γ the Grüneisen constant, T the temperature, and A is a constant that is independent of pressure [36]. If we model the pressure dependence of ω_D through the pressure dependence of the cross-plane elastic constant, i.e., if we assume $\omega_D \propto \sqrt{C_{33}}$, then the prediction of the LS equation is also in good agreement with the data, see Fig. 4. (The Grüneisen constant for longitudinal modes in the cross-plane direction, $\gamma = (1/2)dC_{33}/dP \approx 3.8$, is approximately independent of pressure.) We believe, however, that the good agreement between the data and the LS equation is fortuitous since the LS equation is derived for an isotropic crystal and therefore the scaling $\omega_D \propto \sqrt{C_{33}}$ is difficult to justify.

In conclusion, we have combined the techniques of picosecond interferometry, time-domain thermorefectance, and the diamond anvil cell to investigate the pressure dependence of thermal conductivity at pressures sufficiently high to significantly alter the anisotropy of a prototypical layered crystal, muscovite. The approach we have developed is general and applicable to any material that can be prepared with a smooth surface, coated with a metal film, and loaded into a diamond anvil cell. While these initial studies

are limited to room temperature, we anticipate that the upper temperature range of the measurements will only be limited by the physical and chemical stability of the metal film. The pressure dependence of the cross-plane thermal conductivity of a layered crystal can mostly be accounted for by changes in the cross-plane sound velocities and elastic anisotropy.

This work was supported by the US Air Force Office of Scientific Research Grant No. MURI FA9550-08-1-0407, DOE and Carnegie Institution of Washington (CDAC DOE CI JL 2008 - 05246) and National Aeronautics and Space Administration Grant 655 NASA NNX09AB946. W. -P. H. acknowledges support by the Taiwan Merit Scholarship from National Science Council (NSC-095-SAF-I-564-005-TMS), Taiwan, Republic of China. We thank Barbara Lavina for the help with the gas loading at GeoSoilEnviroCARS (Sector 13), Advanced Photon Source (APS), Argonne National Laboratory. The gas loading system is partially supported by COMPRES.

*whsieh2@illinois.edu

References

- [1] C. Chiritescu *et al.*, *Science* **315**, 351 (2007).
- [2] L. Hu *et al.*, unpublished.
- [3] T. Kanno, S. Yotsuhashi, and H. Adachi, *Appl. Phys. Lett.* **85**, 739 (2004).
- [4] Y. Shen, D. R. Clarke, and P. A. Fuierer, *Appl. Phys. Lett.* **93**, 102907 (2008).
- [5] K. Takahata *et al.*, *Phys. Rev. B* **61**, 12551 (2000).
- [6] I. Terasaki *et al.*, *Phys. Rev. B* **70**, 214106 (2004).
- [7] A. S. Gray, and C. Uher, *J. Materials Science* **12**, 959 (1977).
- [8] R. W. Powell, and E. Griffiths, *Proc. Roy. Soc. London A* **163**, 189 (1937).
- [9] D. Gerlich, *J. Phys. C-Solid State Phys.* **15**, 4305 (1982).
- [10] A. M. Hofmeister, *Proceedings of the National Academy of Sciences of the United States of America* **104**, 9192 (2007).
- [11] S. W. Kieffer, *J. Geophys. Res.* **81**, 3025 (1976).
- [12] S. W. Kieffer, I. C. Getting, and G. C. Kennedy, *J. Geophys. Res.* **81**, 3018 (1976).
- [13] R. G. Ross *et al.*, *Rep. Prog. Phys.* **47**, 1347 (1984).
- [14] E. H. Abramson, J. M. Brown, and L. J. Slutsky, *J. Chem. Phys.* **115**, 10461 (2001).
- [15] Y. Xu *et al.*, *Phys. Earth Planet. Interiors* **143**, 321 (2004).
- [16] P. Beck *et al.*, *Appl. Phys. Lett.* **91**, 181914 (2007).
- [17] H. K. Mao *et al.*, *J. Appl. Phys.* **49**, 3276 (1978).
- [18] M. Rivers *et al.*, *High Pressure Research* **28**, 273 (2008).
- [19] C. A. Paddock, and G. L. Eesley, *J. Appl. Phys.* **60**, 285 (1986).
- [20] D. A. Young *et al.*, in *Phonon Scattering in Condensed Matter*, edited by A. C. Anderson and J. P. Wolfe (Springer, Berlin, 1986).
- [21] D. G. Cahill *et al.*, *J. Appl. Phys.* **93**, 793 (2003).
- [22] K. Kang *et al.*, *Rev. Sci. Instrum.* **79**, 114901 (2008).
- [23] R. G. Dandrea, and N. W. Ashcroft, *Phys. Rev. B* **32**, 6936 (1985).
- [24] D. G. Cahill, *Rev. Sci. Instrum.* **75**, 5119 (2004).
- [25] Z. B. Ge, D. G. Cahill, and P. V. Braun, *Phys. Rev. Lett.* **96**, 186101 (2006).
- [26] K. V. Tretyakov, and S. Scandolo, *J. Chem. Phys.* **121**, 11177 (2004).
- [27] H. Shimizu *et al.*, *Phys. Rev. Lett.* **86**, 4568 (2001).
- [28] W. P. Binnie, *Phys. Rev.* **103**, 579 (1956).
- [29] *Thermophysical properties of high temperature solid materials*, Purdue University, edited by Y. S. Touloukian (1967) **4**.

- [30] C. Bercegeay, and S. Bernard, *Phys. Rev. B* **72**, 214101 (2005).
- [31] R. M. Wentzcovitch *et al.*, *Earth and Planetary Sci. Lett.* **164**, 371 (1998).
- [32] J. Faust, and E. Knittle, *J. Geophys. Res.-Solid Earth* **99**, 19785 (1994).
- [33] K. E. O'Hara, X. Y. Hu, and D. G. Cahill, *J. Appl. Phys.* **90**, 4852 (2001).
- [34] C. Thomsen *et al.*, *Opt. Commun.* **60**, 55 (1986).
- [35] L. E. McNeil, and M. Grimsditch, *J. Phys.-Condensed Matter* **5**, 1681 (1993).
- [36] G. A. Slack, in *Solid State Physics* (Academic, New York, 1979) **34**, 35.

Figure Captions

FIG. 1. Schematic drawing of the pump-probe optical measurements (TDTR and picosecond interferometry) of a muscovite sample in a diamond anvil cell. An Al thin film serves as a transducer that absorbs energy from the pump beam and enables measurements of temperature through changes in optical reflectivity. The pressure medium is Ar.

FIG. 2. (a) Example data for the ratio V_{in}/V_{out} as a function of delay time and fits (solid lines) to the heat flow model of Ref [24]; data and fits are labeled by the pressure. (b) Example data for the oscillations in V_{in} as a function of delay time that are used to measure the Brillouin frequency of muscovite.

FIG. 3. Pressure dependence of the (a) Brillouin frequency and (b) C_{33} of the muscovite. C_{33} is derived from the Brillouin frequency data using the equation of state of muscovite and assuming that the index of refraction follows the Lorentz-Lorenz equation. The estimated $C_{11} = 184 \text{ GPa} + 4P$ and previously measured bulk modulus $B^T = 61.4 \text{ GPa} +$

6.9P [32] are plotted as solid and dashed line, respectively, for comparison.

FIG. 4. Measurements (solid symbol) and theoretical predictions of the cross-plane thermal conductivity Λ of muscovite as a function of pressure. Error bars on the data points are dominated by uncertainties in the parameters in the thermal model used to analyze the data. The predicted Λ based on a constant relaxation time and an anisotropic Debye model (Eq. 1) is shown as a solid line; the prediction of the LS equation using the scaling $\omega_D \propto \sqrt{C_{33}}$ is shown as a dashed line. The dashed-dot line shows the scaling $\Lambda \propto C_{33}$.

Fig. 1

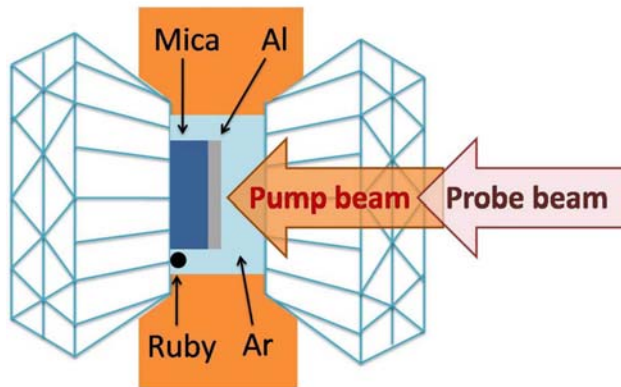


Fig. 2

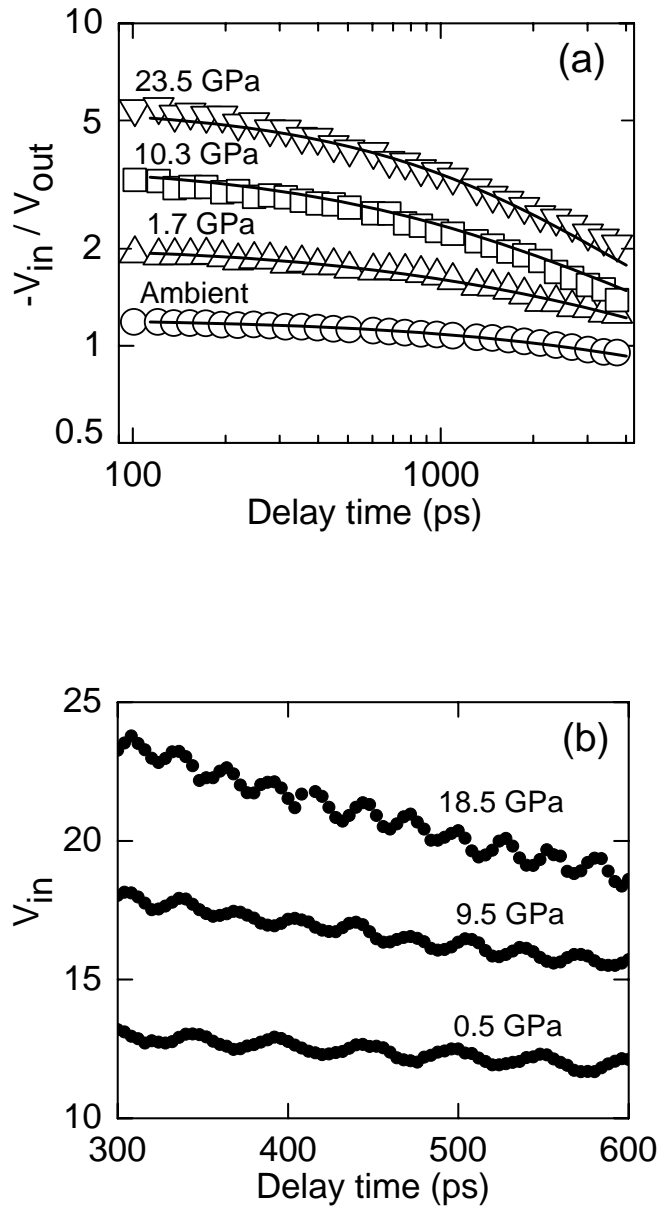


Fig. 3

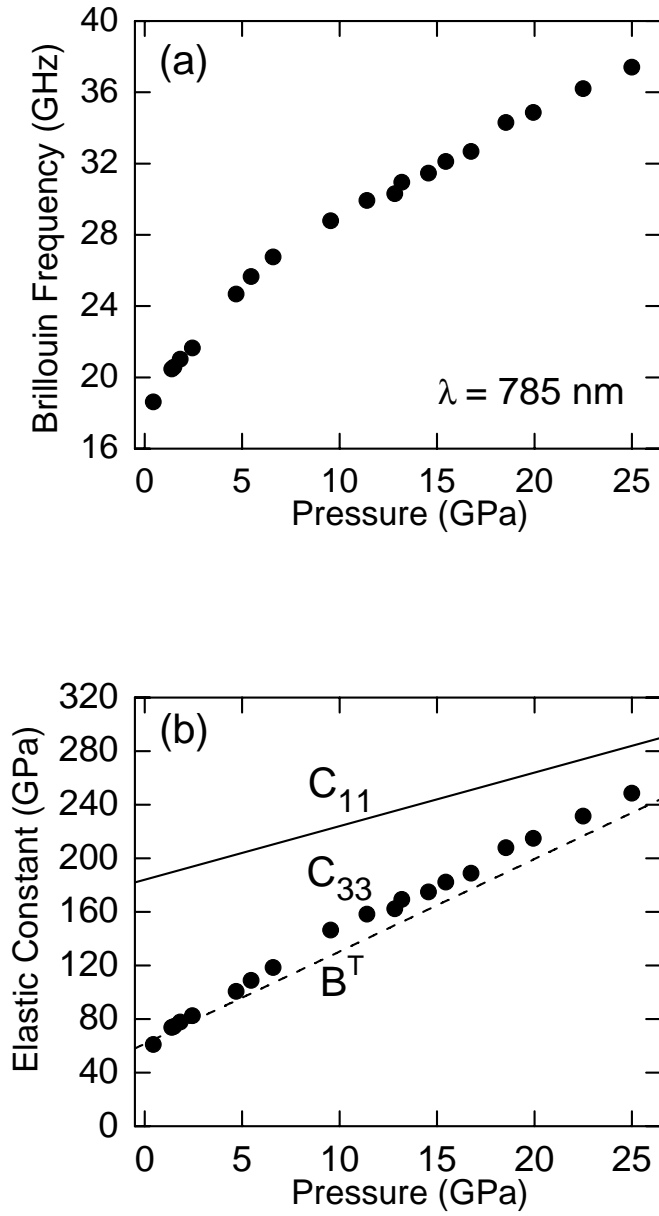


Fig. 4

